

# The tune of the universe: the role of plasma in tests of strong-field gravity

Vitor Cardoso,<sup>1</sup>★ Wen-Di Guo<sup>2,1</sup>† Caio F. B. Macedo,<sup>3</sup>‡ and Paolo Pani,<sup>4</sup>§

<sup>1</sup>*CENTRA, Departamento de Física, Instituto Superior Técnico – IST, Universidade de Lisboa – UL, Avenida Rovisco Pais 1, 1049 Lisboa, Portugal*

<sup>2</sup>*Institute of Theoretical Physics & Research Center of Gravitation, Lanzhou University, Lanzhou 730000, China*

<sup>3</sup>*Faculdade de Física, Universidade Federal do Pará, Salinópolis, Pará, 68721-000 Brazil*

<sup>4</sup>*Dipartimento di Fisica, “Sapienza” Università di Roma & Sezione INFN Roma1, Piazzale Aldo Moro 5, 00185, Roma, Italy*

17 November 2021

## ABSTRACT

Gravitational-wave astronomy, together with precise pulsar timing and long baseline interferometry, is changing our ability to perform tests of fundamental physics with astrophysical observations. Some of these tests are based on electromagnetic probes or electrically charged bodies, and assume an empty universe. However, the cosmos is filled with plasma, a dilute medium which prevents the propagation of low-frequency, small-amplitude electromagnetic waves. We show that the plasma hinders our ability to perform some strong-field gravity tests, in particular: (i) nonlinear plasma effects dramatically quench plasma-driven superradiant instabilities; (ii) the contribution of electromagnetic emission to the inspiral of charged black hole binaries is strongly suppressed; (iii) electromagnetic-driven secondary modes, although present in the spectrum of charged black holes, are excited to negligible amplitude in the gravitational-wave ringdown signal. The last two effects are relevant also in the case of massive fields that propagate in vacuum and can jeopardize tests of modified theories of gravity containing massive degrees of freedom.

**Key words:** Compact binaries; astrophysical medium; dissipative effects in binaries.

## 1 INTRODUCTION

The birth of gravitational-wave (GW) astronomy (Abbott et al. 2019) together with optical/infrared interferometry and radio very large baseline interferometry (Abuter et al. 2018; Akiyama et al. 2019) opened the door to new tests of General Relativity in the strong-field regime. Of special relevance are tests of the black-hole (BH) paradigm, including all the nontrivial general relativistic effects (Yagi & Stein 2016; Barack et al. 2019; Cardoso & Pani 2019). For example, strong evidence for the existence of photon spheres was provided already by LIGO/Virgo (Cardoso & Pani 2019) and by the Event Horizon Telescope (Akiyama et al. 2019). In parallel, strong-field gravity may offer routes to tests of the dark matter content of our universe, turning compact objects into astrophysical particle detectors (Brito et al. 2015; Baumann et al. 2020; Brito et al. 2020).

Several of these tests are directly or indirectly based on electromagnetic (EM) probes or electrically charged objects, and often assume that photons propagate freely in the universe. However, our universe is filled with plasma, a dilute medium which prevents the propagation of low-frequency (and small-amplitude) EM

waves. The scope of this work is to revisit some strong-gravity phenomena to include the crucial effect played by the photon coupling to plasma, and to discuss novel effects that have been so far neglected. We consider constraints on the EM charge of compact objects and plasma-driven superradiant instabilities (Pani & Loeb 2013; Brito et al. 2020; Conlon & Herdeiro 2018), briefly reviewed below. Throughout this manuscript we use geometric units with  $G = c = 1$ .

### 1.1 Constraints on the charge of compact objects

Given that EM fields are ubiquitous and play a key role in most of the known universe, it is only natural to ask whether BHs or other compact objects are endowed with electric charge. Astrophysical BHs are considered to be electrically neutral due to a variety of effects, including electron-positron production and neutralization by the surrounding plasma (Gibbons 1975; Goldreich & Julian 1969; Ruderman & Sutherland 1975; Blandford & Znajek 1977; Barausse et al. 2014, 2015). However, mergers occur in violent conditions – possibly including strong magnetic fields – and sufficiently far away that one may question whether all conditions for neutrality are met (Cardoso et al. 2016; Zajaček et al. 2019). In addition, certain dark matter candidates are (weakly) electrically charged and can circumvent the conditions for neutralization (Cardoso et al. 2016).

Motivated by the potential of GW astronomy to explore these

★ E-mail: vitor.cardoso@ist.utl.pt

† E-mail: wen-di.guo@tecnico.ulisboa.pt

‡ E-mail: caiomacedo@ufpa.br

§ E-mail: paolo.pani@uniroma1.it

issues, the coalescence of charged BH in *electrovacuum* was studied in recent years, both nonlinearly (Zilhão et al. 2012, 2014; Liebling & Palenzuela 2016; Jai-akson et al. 2017; Bozzola & Paschalidis 2019, 2021) and perturbatively in the extreme mass ratio limit (Zhu & Osburn 2018).

Neglecting environmental effects (Barausse et al. 2014, 2015), it was shown that GW observations of the inspiral stage (Cardoso et al. 2016; Christiansen et al. 2020) have the potential to provide interesting constraints on the charge of BHs (Cardoso et al. 2016; Liu et al. 2020; Christiansen et al. 2020). Likewise, the ringdown stage can in principle be used to study the EM charge of the remnant: gravitational and EM modes couple, and the characteristic GW vibration modes of the system contain also a new, EM-like, family of modes, similar to the case of certain modified theories of gravity with extra scalar degrees of freedom nonminimally coupled to gravity (Molina et al. 2010; Blazquez-Salcedo et al. 2016; Okounkova et al. 2017; Witek et al. 2019; Okounkova 2020). Thus, it has been argued that the detection of two or more modes can in principle provide constraints on the mass, spin, and charge of the final BH (Cardoso et al. 2016).

## 1.2 Superradiance and the search for new fundamental fields

Another very concrete example of the discovery potential of BHs and GW astronomy concerns new, fundamental ultralight degrees of freedom. These would render spinning BHs unstable, and lead to a transfer of rotational energy to large-scale condensates in their surroundings; these time-varying structures would then emit quasi-monochromatic GWs, a smoking-gun for new physics (Arvanitaki et al. 2010; Arvanitaki & Dubovsky 2011) (see (Brito et al. 2020) for a review). The mechanism at work in superradiant instabilities requires two key ingredients: an ergoregion that “forces” the field to be dragged along with the compact object, transferring energy and angular momentum to the field (Zel’dovich 1971, 1972; Brito et al. 2020), and a massive bosonic field. The field mass effectively confines the entire setup, therefore turning an energy-extraction mechanism into an instability mechanism (Damour et al. 1976; Detweiler 1980; Brito et al. 2020). For a BH of mass  $M$  and angular momentum  $J = \chi M^2$ , and a vector field of mass  $\hbar\mu$ , such process may be very efficient (Pani et al. 2012a,b; Witek et al. 2013; Endlich & Penco 2017; East 2017; East & Pretorius 2017; Baryakhtar et al. 2017; East 2018; Frolov et al. 2018; Dolan 2018; Siemonsen & East 2020; Baumann et al. 2019); the timescale for BH spin-down – and for the build-up of a massive vector condensate – is controlled by the parameter

$$\gamma = M\mu, \quad (1)$$

and, in the  $\gamma \ll 1$  regime, is of the order (Detweiler 1980; Cardoso & Yoshida 2005; Brito et al. 2020)

$$\tau \sim \frac{M}{\chi\gamma^7} \approx \frac{16}{\chi} \left( \frac{M}{1M_\odot} \right) \left( \frac{0.01}{\gamma} \right)^7 \text{ yr}. \quad (2)$$

The instability is suppressed when the object spins down to  $\chi \sim 2\gamma$ . Stringent constraints on the existence of new particles can then be imposed via (the lack of) observations of GWs emitted by the bosonic condensate that develops around the BH, “gaps” in the mass-spin plane of BHs (Arvanitaki et al. 2010; Arvanitaki & Dubovsky 2011), polarimetry measurements (Plascencia & Urbano 2018), etc, although nonlinear photon effects such as pair production or couplings to Standard Model fields can reduce these bounds (Fukuda & Nakayama 2020; Ikeda et al. 2019; Brito et al.

2020). A complete review of the status of the field is discussed in Ref. (Brito et al. 2020).

Surprisingly, the existence of interstellar plasma permeating the universe could provide an outstanding opportunity to test the existence of ergoregions while simultaneously predicting, or explaining, new phenomena. The interaction between EM waves and ions in a plasma changes the dispersion relation and the effective equations of motion of low-frequency photons (Dendy 1989; Kulsrud & Loeb 1992). The dispersion relation of the photon acquires an effective-mass term given by the plasma frequency (Hora 1991; Kulsrud & Loeb 1992; Pani & Loeb 2013),

$$\omega_p = \sqrt{\frac{e^2 n_e}{\epsilon_0 m_e}} = 1.8 \times 10^3 \left( \frac{n_e}{10^{-3} \text{ cm}^{-3}} \right)^{1/2} \text{ rad s}^{-1}, \quad (3)$$

where  $n_e$  is the electron number density in the plasma, whereas  $m_e$  and  $e$  are the electron mass and charge, respectively, and  $\epsilon_0$  is the vacuum permeability. It is clear from this that the effective mass would be interesting from the point of view of superradiant instabilities of astrophysical systems, since the controlling parameter  $\gamma$  is appreciable (Conlon & Herdeiro 2018),

$$\gamma = \omega_p M \approx 0.09 \left( \frac{\omega_p}{1.8 \times 10^3 \text{ Hz}} \right) \left( \frac{M}{10M_\odot} \right), \quad (4)$$

and therefore the associated instability timescale (2) is relatively small.

Superradiant instabilities in the presence of plasmas have therefore been argued to produce important signatures, including distortions in the cosmic background radiation from primordial BHs (Pani & Loeb 2013), and have been suggested as a possible explanation for Fast Radio Bursts from stellar-size BHs (Conlon & Herdeiro 2018). This has motivated further work on the topic, including the impact of a nonhomogeneous plasma profile around a spinning BH, which reduces the instability rate (Dima & Barausse 2020). It has been also argued that the spin of neutron stars could be limited via the same plasma-driven mechanism (Cardoso et al. 2017), a truly tantalizing prospect to explain the systematic reduction of the spin measured in pulsars compared to the mass-shedding limit.

## 1.3 The role of plasma: shortcomings of previous analyses

Here, we argue that the aforementioned analyses have severe shortcomings, all related to the fact that they neglected some key ingredient in the photon-plasma interaction.

Constraints on the EM charge have so far neglected the fact that plasma is not transparent to low-frequency waves. The balance arguments used to understand how inspiral proceeds breakdown if EM radiation is not being transported to null infinity. Note, in particular, that the plasma reflects any sufficiently low-frequency radiation. For the plasma frequency (3), this corresponds to reflecting back all radiation whose wavelength is *larger* than the binary separation. Thus, the usual boundary conditions involved in the retarded Green’s function change and the nature of the solution is also completely different. This properties of a radiator inside a cavity have been studied from a quantum and classical perspective (Haroche & Raimond 1985; Haroche & Kleppner 1989; Dowling et al. 1991) and support the above view; the radiation can be extremely suppressed or enhanced depending on the cavity and radiator <sup>1</sup>.

<sup>1</sup> We note that the relative size between the cavity and the radiation wavelength is important in the outcome; the boundary conditions are paramount: for absorbing cavities which are much larger than the wavelength of radiation,

Furthermore, previous studies on GW spectroscopy for charged BHs also overlooked environmental effects and how they impact the ringdown stage, in particular they neglected whether the plasma can affect the amplitude of EM-driven quasinormal modes.

Finally, the mechanisms leading to plasma-driven superradiant instabilities neglect backreaction and nonlinear effects. In particular, a small growing electric field will re-arrange the plasma distribution, changing its “effective mass.” In other words, the plasma is assumed to be totally opaque to such low-frequency radiation, but such assumption needs justification, especially for unstable processes in which the EM field initially grows exponentially.

Here, we wish to examine these questions more closely.

## 2 NONLINEAR EFFECTS MAKE PLASMA TRANSPARENT TO RADIATION

Previous studies on plasma-driven BH superradiant instabilities are based on the assumption of a fixed constant plasma density (see Ref. (Dima & Barausse 2020) for an extension to constant, non-homogenous density profiles with a scalar toy model) and, most notably, of weak electric fields. However, relativistic and nonlinear effects cause waves of frequency

$$\omega_p \left( 1 + \frac{e^2 E^2}{m_e^2 \omega^2} \right)^{-1/2} < \omega < \omega_p, \quad (5)$$

to propagate (Kaw & Dawson 1970; Max & Perkins 1971). Here  $E$  is the amplitude of the electric field of the wave. Therefore, when the electric field is weak no frequency  $\omega < \omega_p$  can propagate in the plasma, in agreement with the linear analysis. However, there is a critical electric field

$$E_{\text{crit}} = \frac{m_e}{e} \sqrt{\omega_p^2 - \omega^2}, \quad (6)$$

above which waves with frequency  $\omega$  propagate into the plasma.

When dealing with superradiant instabilities this is a particularly important effect, because the electric field grows exponentially in the initial phase of the instability, before saturating due to nonlinear effects. Indeed, since the dominant superradiant mode has roughly  $\omega \sim \omega_p \left( 1 - \frac{1}{2} \gamma^2 \right)$  (Pani et al. 2012a,b; Pani & Loeb 2013), in the  $\gamma \ll 1$  limit the critical electric field that makes the plasma transparent to this mode is

$$E_{\text{crit}}^{\text{SR}} \sim \frac{m_e}{e} \omega_p \gamma = 0.27 \left( \frac{n_e}{10^{-3} \text{cm}^{-3}} \right)^{1/2} \frac{\gamma}{0.09} \text{ V/m}. \quad (7)$$

Even in the absence of such nonlinear mechanism (but we do not have any reason to speculate on its absence), the assumption that low-frequency EM waves do not propagate in the plasma breaks down when the plasma becomes hot and relativistic, i.e., when the collisional velocity  $\sim 1$ . Since the change in the momentum of one electron over a time  $\Delta t$  is  $\Delta P = F \Delta t$ , we get the critical electric field for this to happen  $E^{\text{rel}} = m_e / (e \Delta \tau)$  with  $\Delta \tau$  the mean collision time between electrons and ions in the plasma. For relativistic electrons,  $\Delta \tau = \ell_e$ , with  $\ell_e = n_e^{-1/3}$  being the mean separation. Therefore, neglecting nonlinear effects the critical value of the electric field above which plasma confinement breaks down reads

$$E_{\text{rel}}^{\text{SR}} = \frac{m_e n_e^{1/3}}{e} = 5 \times 10^6 \left( \frac{n_e}{10^{-3} \text{cm}^{-3}} \right)^{1/3} \text{ V m}^{-1}. \quad (8)$$

tion, the backreaction on the radiator is expected to be negligible; this also is the physical reason why an absorption of photons from, say, the Sun, is not going to affect its emission properties.

When the electric field grows to the above values, the plasma becomes transparent, a burst ensues, and the process starts anew<sup>2</sup>.

One can estimate how much energy is removed from the rotating object in each cycle. The density of energy is  $\sim \epsilon_0 E^2$ , and extended over a spatial distance  $L_{\text{cloud}} \sim 5M/\gamma^2$ , set by the size of the bosonic cloud (Brito et al. 2020). Thus, the total energy in the condensate is

$$U = \epsilon_0 \left( E^{\text{SR}} \right)^2 L_{\text{cloud}}^3, \quad (9)$$

for  $E^{\text{SR}} = E_{\text{crit}}^{\text{SR}}$  or  $E^{\text{SR}} = E_{\text{rel}}^{\text{SR}}$ . On the other hand, the rotational energy of a compact object of radius  $R$  is  $K \sim MR^2 \Omega^2$ , with  $R \sim 2M$  and  $\Omega \gtrsim \gamma/M$ . Using Eq. (7), one finds

$$\begin{aligned} \frac{U}{K} &\lesssim \frac{125 M^2 m_e n_e}{4 \gamma^6} \\ &\approx 9 \times 10^{-39} \left( \frac{M}{10 M_\odot} \right)^2 \left( \frac{n_e}{10^{-3} \text{cm}^{-3}} \right) \left( \frac{0.09}{\gamma} \right)^6. \end{aligned} \quad (10)$$

We note that, even in the absence of the above bound, the threshold (Eq. (8)) at which the plasma becomes transparent under the assumption of relativistic electrons (thus emitting bremsstrahlung radiation and breaking all the assumptions leading to the plasma cutoff frequency) yields

$$\begin{aligned} \frac{U}{K} &\lesssim \frac{125 \epsilon_0 M^2 m_e^2 n_e^{2/3}}{4 \gamma^8 e^2} \\ &\approx 3 \times 10^{-24} \left( \frac{M}{10 M_\odot} \right)^2 \left( \frac{n_e}{10^{-3} \text{cm}^{-3}} \right)^{2/3} \left( \frac{0.09}{\gamma} \right)^8. \end{aligned} \quad (11)$$

Therefore, the above simple analysis shows that relativistic and nonlinear effects hamper dramatically the tapping of rotational energy from a spinning BH. In practice, immediately after the instability occurs the electric field in the BH surroundings becomes large enough as to render the plasma transparent to low-frequency photons, making the trapping (and, in turn, the whole instability) inefficient.

## 3 PLASMAS AND MERGING CHARGED BHs

As previously mentioned, several mechanisms contribute to the neutralization of BHs. For example, charged BHs are quickly discharged by Hawking radiation or by pair-production. In addition, a small amount of external plasma with total mass  $M_{\text{plasma}} \sim 10^{-18} M$  is sufficient to discharge a BH on a short timescale  $\tau \sim 10^{-11} \text{ yr}$  (Cardoso et al. 2016). Neutralization from surrounding plasma would normally screen charge on a Debye lengthscale: the charge of a BH is effectively screened on the spatial scale (exceptions to this rule may occur with stars, but not with objects without atmospheres (Bally & Harrison 1978))

$$\lambda_D = \sqrt{\frac{\epsilon_0 k_B T}{n_e e^2}} \approx 2 \left( \frac{T}{10^6 \text{ K}} \right)^{1/2} \left( \frac{10^{-3} \text{cm}^{-3}}{n_e} \right)^{1/2} \text{ km}. \quad (12)$$

Colder or denser media yield even tighter atmospheres. Thus, for all practical purposes BHs surrounded by plasmas are neutral.

<sup>2</sup> We note that the electric field of this radiation burst decreases with distance; for large enough distances the plasma will again be opaque to it; however, this is a subdominant effect in this process, and its overall consequence is to provide the plasma with a small – and irrelevant for our discussion – effective mass.

In the eventuality that the near-horizon region is plasma-depleted and that neutralization does not occur, then two BHs can indeed be orbiting each other and emit EM radiation. However, also in this case the plasma surrounding the binary strongly hampers EM emission, as discussed in the next section.

### 3.1 The inspiral phase

The low-frequency, nearly Newtonian stage in the life of a binary of two compact objects provides stringent constraints on the gravity theory and possible new interactions (Will 2014; Yagi & Stein 2016). The underlying mechanism is as follows. Compact objects such as neutron stars or BHs on tight orbits dissipate energy mostly through GW emission. Mass loss via winds, tidal acceleration, or friction with the environment are all negligible in comparison. In these circumstances, the energy loss can be computed using numerical methods or a post-Newtonian expansion. It is found that GW emission quickly circularizes the orbit (Peters 1964). It is thus customary to assume that the two orbiting objects are on quasi-circular orbits. To lowest order in the orbital velocity, the energy loss is given by the quadrupole formula

$$\frac{d\mathcal{E}_{\text{rad}}^{\text{grav}}}{dt} = -\frac{32}{5} \frac{m_1^2 m_2^2 (m_1 + m_2)}{L^5}, \quad (13)$$

where  $L$  is the orbital radius and  $m_i$  is the mass of the  $i$ -th body. On the other hand, energy loss to radiation triggers an evolution of the binary parameters. In particular, this can be obtained using a quasi-adiabatic approximation to evolve the otherwise constants of motion such as the binary's energy and angular momentum. Such evolution can be determined using the expression for the orbital energy

$$\mathcal{E}_{\text{orb}} = -\frac{m_1 m_2}{2L}, \quad (14)$$

equating  $d\mathcal{E}_{\text{orb}}/dt$  to  $d\mathcal{E}_{\text{rad}}/dt$  and promoting the orbital radius  $L$  to be a function of time.

New physics will impact both the emission of radiation, changing Eq. (13), and the orbital relation (14). For example, if the objects carry electric charge there is emission of mostly dipolar EM waves in addition to (mostly quadrupolar) GW emission. When the charge-to-mass ratio is small, dipolar radiation is of the order (Cardoso et al. 2016; Liu et al. 2020; Christiansen et al. 2020)

$$\frac{d\mathcal{E}_{\text{rad}}^{\text{elec}}}{dt} = -\frac{2}{3} \left( \frac{Q_1}{m_1} - \frac{Q_2}{m_2} \right)^2 \frac{m_1^2 m_2^2}{4\pi\epsilon_0 L^4}, \quad (15)$$

where  $Q_i$  is the charge of the  $i$ -th body. Thus, EM emission dominates at separations larger than

$$L_{\text{crit}} = \frac{48M_{\text{tot}}}{5(\delta_1 - \delta_2)^2}, \quad (16)$$

where  $M_{\text{tot}} = m_1 + m_2$  and  $\delta_i = Q_i/(\sqrt{4\pi\epsilon_0}m_i) < 1$  is the charge-to-mass ratio of the  $i$ -th body. For binaries at separation  $L \gtrsim L_{\text{crit}}$  the EM emission causes a distinct evolution of the orbital phase as time progresses. These effects have been used to impose stringent constraints on the charge of the inspiralling objects (Cardoso et al. 2016; Christiansen et al. 2020; Bozzola & Paschalidis 2021).

Unfortunately, the Larmor result (15) is valid in electrovacuum, but not in the presence of a plasma. It can be immediately recognized that the plasma frequency (3) is much larger than the orbital frequency of astrophysical BHs or neutron stars, especially in the relevant regime when  $L \gtrsim L_{\text{crit}}$ . Thus, the assumption that the generated waves are able to travel freely and contribute to energy

loss is incorrect. In fact, the entire calculation underlying (15), in particular the imposition of Sommerfeld conditions at infinity, is not justified.

Is it possible that, just like the superradiance clouds in the previous section, photons are still able to tunnel through via nonlinear effects? We now show that this is not possible. Take a pointlike mass  $m_i$ , carrying charge  $Q_i$ , in motion with acceleration  $a$ . Assuming Sommerfeld conditions at infinity, the electric field at distance  $r$  in the wave zone is of order (Jackson 1999)

$$E = \frac{Q_i}{4\pi\epsilon_0} \frac{a}{r}. \quad (17)$$

When the motion is circular and dictated by the inverse-square law, then  $a \sim \Omega^2 L$ , with  $\Omega = \sqrt{M_{\text{tot}}/L^3}$  being the Keplerian frequency. For simplicity we assume that the binary components are weakly charged, so that the acceleration is mostly provided by gravity (the calculation generalizes trivially). Thus, at small  $r$  the electric field is large and possibly larger than the critical field for transparency which, to be conservative, can be assumed to be the largest value among those discussed in the previous section, i.e. Eq. (6). Taking into account the typical plasma frequency (3), one concludes that  $\omega \ll \omega_p$  during the inspiral of astrophysical BHs, especially in the large-separation regime where the dipolar terms arising from EM emission could dominate (i.e.,  $L > L_{\text{crit}}$ ). Thus, one finds the distance  $r_{\text{crit}}$  below which the electric field of the radiation is larger than  $E_{\text{crit}}$ ,

$$r_{\text{crit}} \approx \delta_i \delta_e \left( \frac{M_{\text{tot}}}{L} \right)^2 \frac{1}{\omega_p}, \quad (18)$$

where  $\delta_e \approx 2 \times 10^{21}$  is the electron charge-to-mass ratio and for simplicity we assumed equal mass ratio, i.e.  $M \approx M_{\text{tot}}/2$ . By evaluating the above formula at  $L \approx L_{\text{crit}}$  (Eq. (16)), and using Eq. (3), we obtain

$$\frac{r_{\text{crit}}}{\lambda} \approx 10^{19} \delta_i (\delta_1 - \delta_2)^7 \left( \frac{M_{\odot}}{M_{\text{tot}}} \right) \quad (19)$$

where  $\lambda = 2\pi/\Omega$  is the radiation wavelength at  $L = L_{\text{crit}}$ . Note the strong dependence on the charge-to-mass ratios  $\delta_i$ 's and the fact that  $r_{\text{crit}} = 0$  if  $\delta_1 = \delta_2$ , since in this case dipolar emission is suppressed. For supermassive BHs ( $M_{\text{tot}} \approx 10^6 M_{\odot}$ ), one finds  $\frac{r_{\text{crit}}}{\lambda} \lesssim 1$  whenever  $\delta_i = \mathcal{O}(0.01)$  or smaller. In other words, in the radiation zone, the electric field is always sub-critical. This means that the plasma is *not* transparent to this radiation. For stellar-mass BHs or for larger  $\delta_i$ 's, the ratio  $r_{\text{crit}}/\lambda$  can be larger by orders of magnitude. Nevertheless, notice that plasma is not only absorbing, but also actually reflecting radiation. As we remarked in footnote 1, such aspect is crucial in the dynamics of objects within cavities: within a corresponding number of cycles the radiation would have reflected off and interacted with the binary, affecting its dynamics.

Finally, the above calculation and argument may also apply, in principle, to interactions other than the EM one. Take for example some “hidden” vector  $V^\mu$  field coupled to the Maxwell sector (Cardoso et al. 2016). In such a case, interstellar (charged) dark matter and standard interstellar plasma would both work to provide an effective mass to the propagating field  $V^\mu$ , possibly turning the interstellar plasma opaque to radiation, thereby suppressing emission in the dark sector. However, the effective mass for the dark sector is dependent on the coupling and on the mass of the carriers. Therefore, the above constraints may be evaded in some beyond-Standard-Model scenarios.

To summarize, the use of EM dipolar losses [Eq. (15)] to constrain the charge (EM or even possibly of some other “dark” interaction) of astrophysical objects is not justified. Careful understanding



of the role of plasma is necessary, but not available at this point. Indeed, the problem of two orbiting charged particles in a plasma shares some similarities with that of two particles in a perfectly reflecting box. In the latter case energy cannot be radiated to infinity and stationary solutions where the orbit does not shrink exist (see, e.g., Ref. (Dias et al. 2012) for the case of a binary in asymptotically anti de-Sitter spacetime). However, the case of the plasma is much more complex since: i) the reflection of the radiation is frequency dependent; and ii) as discussed before plasma is opaque only at the linear level, in reality we expect both the radiation and the binary motion to affect the plasma dynamics and profile around the binary, potentially modifying the propagation/absorption of EM waves.

### 3.2 The ringdown stage

The existence of couplings between two fields introduces mixing of modes in the ringdown. In the context of collisions of two charged BHs, gravitational and EM perturbations are coupled to each other. This leads to mode mixing in the ringdown, which is described by gravitational-led and EM-led modes. The former (resp., latter) are those that correspond to the standard gravitational (resp., EM) modes of a Reissner-Nordstrom BH in the neutral limit ( $Q \rightarrow 0$ ). We illustrate this effect in Appendix A, where we overview the collision of two electrically charged BHs within a perturbative approach. The effect is more pronounced when the coupling between the two sectors is large, which in the case of electrically charged BHs is related to the product of their charges.

To take plasma physics into account demands a more careful analysis, as one should consider the perturbations induced by the matter surrounding each BH and possibly the binary as a whole. We are currently unable to deal with this problem in full generality, which would require the analysis of plasma physics in the curved spacetime near a BH. However, we are interested in understanding one particular and crucial aspect of plasma physics, which is the introduction of an effective mass for the photon. The simplest toy model to mimic this scenario should be a massive vector coupled to a charged BH. Unfortunately, there are no BH solutions in Einstein-Proca theory (Bekenstein 1972a,b), which makes even this toy model uninteresting. We can get a grasp into the qualitative aspects of the problem by investigating another proxy toy model, in which two fields are coupled together with a large (possibly effective) mass term.

#### 3.2.1 Toy model

We wish to study how does spacetime react when couplings to (possibly effective) massive fields are considered. Following the discussions presented in the previous section, this is precisely what happens when plasma is present in the surroundings of BHs. Our prototype model, which presents the main desired features, is dynamical Chern-Simons theory with a self-interacting potential (Alexander 2005). In this theory the axial gravitational perturbations couple to a (pseudo)scalar field. The similarities between the physics of plasmas and the dynamical Chern-Simons theory come from the fact that both theories contain a field coupled to the gravitational one (a Maxwell field in the plasma case, and a scalar field in Chern-Simons gravity, respectively) and both feature a trapping mechanism due to the masses of these fields. The scalar-field mass is analogous to the effective mass provided by the plasma frequency. The strength of the coupling in the dynamical Chern-Simons case is controlled by a theory parameter, while in the plasma scenario is related to the BH charge.

The action of the dynamical Chern-Simons theory is

$$S = \kappa \int d^4x \sqrt{-g} R + \frac{\alpha}{4} \int d^4x \sqrt{-g} \vartheta *RR - \frac{\beta}{2} \int d^4x \sqrt{-g} [g^{ab} \nabla_a \vartheta \nabla_b \vartheta + V(\vartheta)] + S_{\text{mat}}, \quad (20)$$

where  $\vartheta$  is the scalar field coupled to gravity, and

$$*RR = \frac{1}{2} R_{abcd} \epsilon^{baef} R^{cd}{}_{ef} \quad (21)$$

is the Pontryagin term. The equation of motion can be obtained by varying the action with respect to the metric  $g_{ab}$  and the scalar field  $\vartheta$ , namely:

$$G_{ab} + \frac{\alpha}{\kappa} C_{ab} - \frac{1}{2\kappa} T^{\vartheta}{}_{ab} = \frac{1}{2\kappa} T_{ab}, \quad (22)$$

$$\square \vartheta - \frac{dV}{d\vartheta} = -\frac{\alpha}{4\beta} *RR, \quad (23)$$

where  $G_{ab} = R_{ab} - \frac{1}{2} g_{ab} R$  is the Einstein tensor,  $T^{\vartheta}{}_{ab} = \beta [\vartheta_{;a} \vartheta_{;b} - \frac{1}{2} g_{ab} \square \vartheta - g_{ab} V(\vartheta)]$ ,  $\square = g^{ab} \nabla_a \nabla_b$  is the D'Alembertian operator, and

$$C^{ab} = \vartheta_{;c} \epsilon^{cde(a} \nabla_e R^{b)}{}_d + \vartheta_{;cd} *R^{d(ab)c}, \quad (24)$$

where  $\vartheta_{;a} = \nabla_a \vartheta$ ,  $\vartheta_{;ab} = \nabla_a \nabla_b \vartheta$ , and  $*R^{abcd} = \frac{1}{2} \epsilon^{cdef} R^{ab}{}_{ef}$ . In the geometric units adopted so far,  $\kappa = 1/16\pi$ .

For concreteness, we consider the simplest potential for a massive scalar field,

$$V(\vartheta) = \frac{\mu^2}{2} \vartheta^2, \quad (25)$$

where  $\mu\hbar$  is the mass of the scalar.

We consider a spherically symmetric background, which is described by the Schwarzschild solution also in this theory. Gravitational perturbations on this background can be expanded in a basis of (scalar, vector, and tensor) spherical harmonics (Regge & Wheeler 1957; Zerilli 1970; Chandrasekhar 1983). The scalar field can be expanded in scalar spherical harmonics as follows

$$\vartheta = \frac{\Theta^{lm}}{r} Y^{lm} e^{-i\omega t}. \quad (26)$$

While the polar (Zerilli) sector is the same as in General Relativity and reduced to a single, second-order, radial differential equation (Zerilli 1970; Chandrasekhar 1983), the axial (Regge-Wheeler) sector is coupled to scalar perturbation and reduces to the system (Molina et al. 2010) (we omit for simplicity the indices  $l$  and  $m$  in the variables  $\Psi$  and  $\Theta$ ),

$$\frac{d^2}{dr_{\star}^2} \Psi + (\omega^2 - V_{11}) \Psi = V_{12} \Theta, \quad (27)$$

$$\frac{d^2}{dr_{\star}^2} \Theta + (\omega^2 - V_{22}) \Theta = V_{21} \Psi, \quad (28)$$

where we have defined<sup>3</sup>

$$V_{11} = f(r) \left[ \frac{l(l+1)}{r^2} - \frac{6M}{r^3} \right], \quad (29)$$

$$V_{12} = f(r) \frac{96\pi M}{r^5}, \quad (30)$$

$$V_{21} = f(r) \frac{6M(l+2)!}{r^5 \beta(l-2)!}, \quad (31)$$

$$V_{22} = f(r) \left[ \frac{l(l+1)}{r^2} \left( 1 + \frac{576\pi M^2}{\beta r^6} \right) + \frac{2M}{r^3} + \mu^2 \right], \quad (32)$$

with  $f(r) = 1 - 2M/r$ , and  $r_\star = r + 2M \ln(r/2M - 1)$  being the tortoise coordinate. In the above,  $\Psi$  is the Fourier-transform of the Regge-Wheeler master function, itself a combination of (axial-like) metric fluctuations (Zerilli 1970; Chandrasekhar 1983; Molina et al. 2010).

From the above equations, one immediately sees that the scalar perturbations source the gravitational ones with a relative coupling  $\propto \Theta/\Psi$ , whereas the gravitational perturbations source the scalar ones with a relative coupling  $\propto \Psi/(\beta\Theta)$ . Therefore, when  $\beta$  is small (large), the scalar field is strongly (weakly) sourced by the gravitational perturbation, while the latter depends on  $\beta$  only indirectly through the value of  $\Theta$ .

When using such Chern-Simons theory to understand plasmas around Schwarzschild BHs, one needs to control the couplings  $M\mu$  and  $\tilde{\beta} \equiv \beta M^4$ . The mass coupling parameter  $M\mu$  depends on the environmental plasma, and can be estimated from Eq. (4). The coupling  $\beta$  in Eqs. (27)–(28) can be estimated by considering how charged perturbations couple to gravity. This coupling is insensitive to the plasma and should be well described by the Einstein-Maxwell theory, which we understand well. The relevant perturbation equations can be separated and decoupled, and reduced to the form of Eqs. (27)–(28) (Cardoso et al. 2016). We find a coupling  $\tilde{\beta} \sim M^2/Q^2 \geq 1$ . Thus,  $\tilde{\beta} = 100, 1$ , correspond respectively to  $Q = 0.1, 1M$ . These values are representative of the constraints that could in principle be achieved with GW astronomy, as reported in previous work (Cardoso et al. 2016).

### 3.2.2 Numerical procedure

We have studied Eqs. (27)–(28) with two different methods. In particular, we used established techniques to look for the characteristic modes (quasinormal modes) of such a system in the frequency domain (Berti et al. 2009; Pani 2013). These frequencies tell us how fluctuations decay at very late times. However, such a knowledge is insufficient, if not accompanied by the relative amplitudes of such fields. To understand this aspect, we also performed evolutions of the corresponding 1+1 partial differential equations: following Refs. (Molina et al. 2010; Macedo 2018), we use the light-cone coordinates,  $u = t - r_\star$  and  $v = t + r_\star$ . Then, the field equations can be written in matricial form as  $4 \frac{\partial^2}{\partial u \partial v} \Phi = -V\Phi$ , with

$$\Phi = \begin{pmatrix} \Psi \\ \Theta \end{pmatrix}, \quad V = \begin{pmatrix} V_{11} & V_{12} \\ V_{21} & V_{22} \end{pmatrix}. \quad (33)$$

We consider three different initial data  $\text{ID}_{2,\Psi,\Theta}$  of the form

$$\Phi(0, v) = \begin{pmatrix} \epsilon_\Psi e^{-(v-v_c)^2/2\sigma} \\ \epsilon_\Theta e^{-(v-v_c)^2/2\sigma} \end{pmatrix}, \quad \Phi(u, 0) = \begin{pmatrix} 0 \\ 0 \end{pmatrix},$$

<sup>3</sup> It is worth noting that the couplings  $\alpha$  and  $\beta$  are degenerate and one of them can be set to unity without loss of generality (Molina et al. 2010). We use this freedom to fix  $\alpha = 1$  and keep  $\beta$  as a free parameter.

with  $(\epsilon_\Psi, \epsilon_\Theta) = (1, 1), (1, 0), (0, 1)$  for  $\text{ID}_2, \text{ID}_\Psi, \text{ID}_\Theta$ , respectively. In other words,  $\text{ID}_2$  corresponds to both fields initially perturbed, whereas  $\text{ID}_\Psi$  and  $\text{ID}_\Theta$  correspond to only  $\Psi$  or only  $\Theta$  initially perturbed, respectively. We focus on width  $\sigma/M = 1$  and a Gaussian located at  $v_c/M = 10$ . The ranges of  $u$  and  $v$  are both  $(0, 400M)$ , and we extract the data at  $r_\star = 50M$ .

### 3.2.3 Results

For  $\tilde{\beta} = 100$ , a frequency-domain analysis of the quadrupole modes with  $l = 2$  and mass coupling  $M\mu = 0.1$  indicates the presence of various characteristic modes. One is located at  $M\omega \sim 0.369 - 0.092i$  and can be identified with a gravitational-led mode. In the decoupled  $\tilde{\beta} \rightarrow \infty$  limit, this is the lowest and dominant gravitational quasinormal mode (Berti et al. 2009; Macedo rdw). A second dominant mode is located at  $M\omega \sim 0.506 - 0.094i$  which in the massless decoupled limit is the lowest quasinormal frequency of a minimally coupled scalar field. For  $\tilde{\beta} = 1$  the modes' frequencies change. The lowest gravitational-driven mode is at  $0.29 - 0.098i$ , while the scalar-driven goes up substantially to  $M\omega \sim 1.4 - 0.14i$ .

A mass term gives rise to new late-time phenomena, in particular the appearance of quasi-bound, Hydrogen-like states (Detweiler 1980; Brito et al. 2020; Macedo 2018). These are followed by late-time power-law tails, triggered by back-scattering off spacetime curvature (Price 1972; Hod & Piran 1998; Koyama & Tomimatsu 2001, 2002; Witek et al. 2013). For massless fields, the late-time power law tail is of the form  $\Psi \sim t^{-(2l+3)}$  for scalars, for example (Price 1972; Witek et al. 2013). For massive fields, these tails have the form  $t^p \sin \mu t$ , with  $p = -(l + 3/2), -5/6$  at intermediate and late times, respectively. The quasi-bound state and tail phase can be seen to take over after  $t \sim 250M$  in the top panels of Fig. 1. Note that the very late-time behavior of massless fields is markedly different, as we remarked it is a pure power-law decay. We will not consider this stage in great detail, since we are mostly interested in the initial ringdown stage. For  $\tilde{\beta} = 100$  and  $\mu = 0.1$  we find  $M\omega \sim 0.0999 - 2 \times 10^{-17}i$ . In general this mode is characterized by  $\text{Re}(\omega) \sim \mu$ . The quasi-bound state for  $\tilde{\beta} = 1$  remains at  $\omega \sim \mu$ , with the imaginary part increasing (Macedo 2018).

To which extent are these modes excited during the evolution of our initial conditions? The outcome of the time evolutions are summarized in Fig. 1 (for  $\tilde{\beta} = 100$ ) and Fig. 2 (for  $\tilde{\beta} = 1$ ) for different mass couplings  $M\mu$ . The left, middle, and right columns correspond to  $\text{ID}_2, \text{ID}_\Psi, \text{ID}_\Theta$ , respectively, whereas the top (bottom) two rows correspond to zero or small (large) values of the scalar mass coupling  $\mu M$ .

Although we show the evolution of both the scalar and the gravitational field, for the purpose of this discussion let us focus on the gravitational sector alone, the first and third row in Figs. 1 - 2. The first aspect that stands out is that, in general, the new channel – the scalar – has an impact also in the gravitational sector. The evolution of the gravitational field leads to a ringdown stage which is not a simple damped sinusoid, but a superposition of at least two of the modes discussed above. Thus, the scalar quasinormal mode percolates to the gravitational sector due to the coupling. Furthermore, for massive scalar field, the very late time behavior of the gravitational sector is that of a weakly damped sinusoid controlled by the scalar quasi-bound states, ringing at a frequency  $\omega \sim \mu$  (Macedo 2018).

However, our results show that

- (i) The *amplitude* of the scalar-driven quasinormal mode in the gravitational sector is smaller at smaller couplings (large  $\beta$ ). This is also apparent from the panels in Figs. 1 - 2.

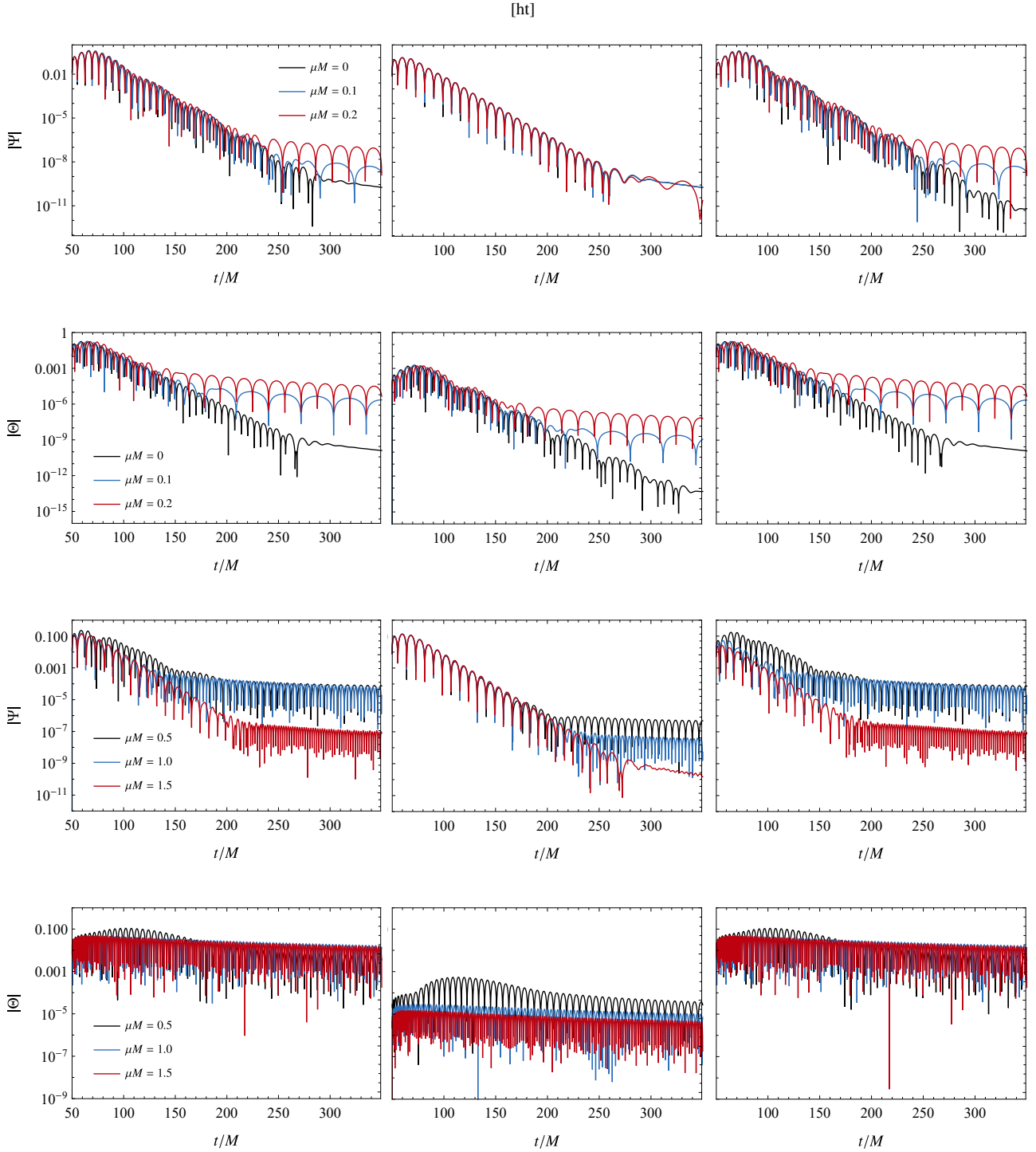


**Figure 1.** Ringdown time evolution in our toy model in which a massive scalar field  $\Theta$  is coupled to axial gravitational perturbations  $\Psi$ . We consider  $\tilde{\beta} = 100$  (small coupling) and the initial data is located at  $v_c = 10$ . The top two rows refer to  $\mu M = 0, 0.1, 0.2$  (zero or small mass term), whereas the bottom two rows correspond to  $\mu M = 0.5, 1, 1.5$  (moderately large mass term). From left to right:  $ID_2$ ,  $ID_\Psi$ ,  $ID_\Theta$ . In all cases we set  $\alpha = 1$ .

(ii) More importantly, *at small couplings and large masses* the gravitational ringdown is universal. To a good approximation it corresponds to the modes of BHs in vacuum GR. This is depicted in the third row, second column of Fig. 1. Increasing the mass term  $M\mu$  delays the appearance of the quasi-bound state dominance, where

the field rings at  $\omega \sim \mu$ , a clear imprint from the scalar sector in the gravitational waveform. Notice that even at large couplings this feature is present: the larger the mass  $M\mu$  the more pure and scalar-free is the gravitational waveform. As in the rest of this work, this

feature arises because the scalar is unable to propagate and therefore the equations decouple in practice.

(iii) The above behavior holds well even when initially there is only a scalar field, such as in the third row, third column of Figs. 1 and 2. The “contamination” of the gravitational wave by the scalar mode is smaller at large mass couplings. In other words, for large  $M\mu$  the amplitude of the induced EM-led, gravitational mode is small and decreases when  $M\mu$  increases.

#### 4 CONCLUSIONS

Recent years have witnessed new developments in strong-field tests of gravity based on charged binaries (Zilhão et al. 2012, 2014; Cardoso et al. 2016; Liebling & Palenzuela 2016; Jai-akson et al. 2017; Zhu & Osburn 2018; Bozzola & Paschalidis 2019, 2021; Christiansen et al. 2020) and on plasma-driven superradiant effects (Pani & Loeb 2013; Conlon & Herdeiro 2018; Dima & Barausse 2020). These tests either neglect the effect of plasma surrounding the binaries, or neglect nonlinear plasma-photon interactions, or anyway treat the photon-plasma coupling in a simplistic way. Unfortunately, as shown in this work, EM emission from binary coalescence, secondary EM-driven modes in the ringdown, and plasma-driven instabilities are strongly suppressed when a more rigorous treatment is performed.

We argue that previous constraints and effects should be revised on the light of our results, and urge for a more detailed treatment of the photon-plasma interactions in strongly-gravitating systems, which is unavailable at the moment. Given the variety of scales and the complex physics involved, full numerical simulations using general-relativistic magneto-hydrodynamics might be required.

Although the main focus of this work was on plasma physics, some of our results are also relevant for tests of modified gravity (Berti et al. 2015). In particular, the suppression of the extra modes in the ringdown and of the dipolar emission in the inspiral should qualitatively apply also to the case of extra fundamental massive fields that propagate in vacuum. While it is well-known that a massive field suppresses the emission of low-frequency waves (see, e.g., Ref. (Cardoso et al. 2011; Yunes et al. 2012; Alsing et al. 2012; Cardoso et al. 2013b,a; Ramazanoğlu & Pretorius 2016) for examples in scalar-tensor theory), we also predict that if the field is massive enough its modes – while present in the spectrum of a BH remnant – cannot be sufficiently excited during the merger and are, therefore, undetectable. It is interesting that the relevant parameter for these effects is typically the coupling  $\mu M$ , which is huge for astrophysical BHs and the typical masses of particles in the standard model<sup>4</sup>. Therefore, if a putative extra fundamental field is massive (approximately with mass  $\mu\hbar \gtrsim 10^{-10}$  eV so that  $\mu M \gtrsim 1$  for a stellar-mass BH) its effects in the inspiral and ringdown are strongly suppressed.

After submission of this work, the effects of plasma on the development of superradiant instabilities was also studied, from different viewpoints, in Refs. (Blas & Witte 2020a,b).

#### ACKNOWLEDGEMENTS

We are indebted to Luis O. Silva and Jorge Vieira for discussions on the physics of plasmas, and for a number of useful references.

<sup>4</sup> For example,  $\mu M \approx 7 \times 10^9$  for a particle as light as  $\mu\hbar = 1$  eV and a stellar-mass BH.

We thank Lang Liu and Rodrigo Vicente for useful feedback. V. C. would like to thank Waseda University for warm hospitality and support while this work was finalized. V. C. acknowledges financial support provided under the European Union’s H2020 ERC Consolidator Grant “Matter and strong-field gravity: New frontiers in Einstein’s theory” grant agreement no. MaGrATh-646597. W. D. Guo acknowledges the financial support provided by the scholarship granted by the Chinese Scholarship Council (CSC) and the Fundamental Research Funds for the Central Universities (Grants Nos. lzujbky-2019-it21). C.F.B.M acknowledges Conselho Nacional de Desenvolvimento Científico e Tecnológico (CNPq), and Coordenação de Aperfeiçoamento de Pessoal de Nível Superior (CAPES), from Brazil. P.P. acknowledges financial support provided under the European Union’s H2020 ERC, Starting Grant agreement no. DarkGRA-757480, and under the MIUR PRIN and FARE programmes (GW-NEXT, CUP: B84I20000100001), and support from the Amaldi Research Center funded by the MIUR program “Dipartimento di Eccellenza” (CUP: B81I18001170001). This project has received funding from the European Union’s Horizon 2020 research and innovation programme under the Marie Skłodowska-Curie grant agreement No 690904. We thank FCT for financial support through Project No. UIDB/00099/2020 and through grant PTDC/MAT-APL/30043/2017. The authors would like to acknowledge networking support by the GWverse COST Action CA16104, “Black holes, gravitational waves and fundamental physics.”

#### DATA AVAILABILITY

The data underlying this article will be shared on reasonable request to the corresponding author.

#### REFERENCES

- Abbott B. P., et al., 2019, *Phys. Rev.*, X9, 031040
- Abuter R., et al., 2018, *A&A*, 618, L10
- Akiyama K., et al., 2019, *Astrophys. J.*, 875, L1
- Alexander T., 2005, *Phys. Rept.*, 419, 65
- Alsing J., Berti E., Will C. M., Zaglauer H., 2012, *Phys. Rev. D*, 85, 064041
- Arvanitaki A., Dubovsky S., 2011, *Phys. Rev.*, D83, 044026
- Arvanitaki A., Dimopoulos S., Dubovsky S., Kaloper N., March-Russell J., 2010, *Phys. Rev.*, D81, 123530
- Bally J., Harrison E. R., 1978, *ApJ*, 220, 743
- Barack L., et al., 2019, *Class. Quant. Grav.*, 36, 143001
- Barausse E., Cardoso V., Pani P., 2014, *Phys. Rev.*, D89, 104059
- Barausse E., Cardoso V., Pani P., 2015, *J. Phys. Conf. Ser.*, 610, 012044
- Baryakhtar M., Lasenby R., Teo M., 2017, *Phys. Rev.*, D96, 035019
- Baumann D., Chia H. S., Stout J., ter Haar L., 2019, *JCAP*, 12, 006
- Baumann D., Chia H. S., Porto R. A., Stout J., 2020, *Phys. Rev. D*, 101, 083019
- Bekenstein J. D., 1972a, *Phys. Rev. D*, 5, 1239
- Bekenstein J., 1972b, *Phys. Rev. D*, 5, 2403
- Berti E., Cardoso V., Starinets A. O., 2009, *Class. Quantum Grav.*, 26, 163001
- Berti E., et al., 2015, *Class. Quant. Grav.*, 32, 243001
- Blandford R., Znajek R., 1977, *Mon. Not. Roy. Astron. Soc.*, 179, 433
- Blas D., Witte S. J., 2020a, *Phys. Rev. D*, 102, 123018
- Blas D., Witte S. J., 2020b, *Phys. Rev. D*, 102, 103018
- Blazquez-Salcedo J. L., Macedo C. F. B., Cardoso V., Ferrari V., Gualtieri L., Khoo F. S., Kunz J., Pani P., 2016, *Phys. Rev.*, D94, 104024
- Bozzola G., Paschalidis V., 2019, *Phys. Rev.*, D99, 104044
- Bozzola G., Paschalidis V., 2021, *Phys. Rev. Lett.*, 126, 041103
- Brito R., Cardoso V., Pani P., 2015, *Class. Quant. Grav.*, 32, 134001



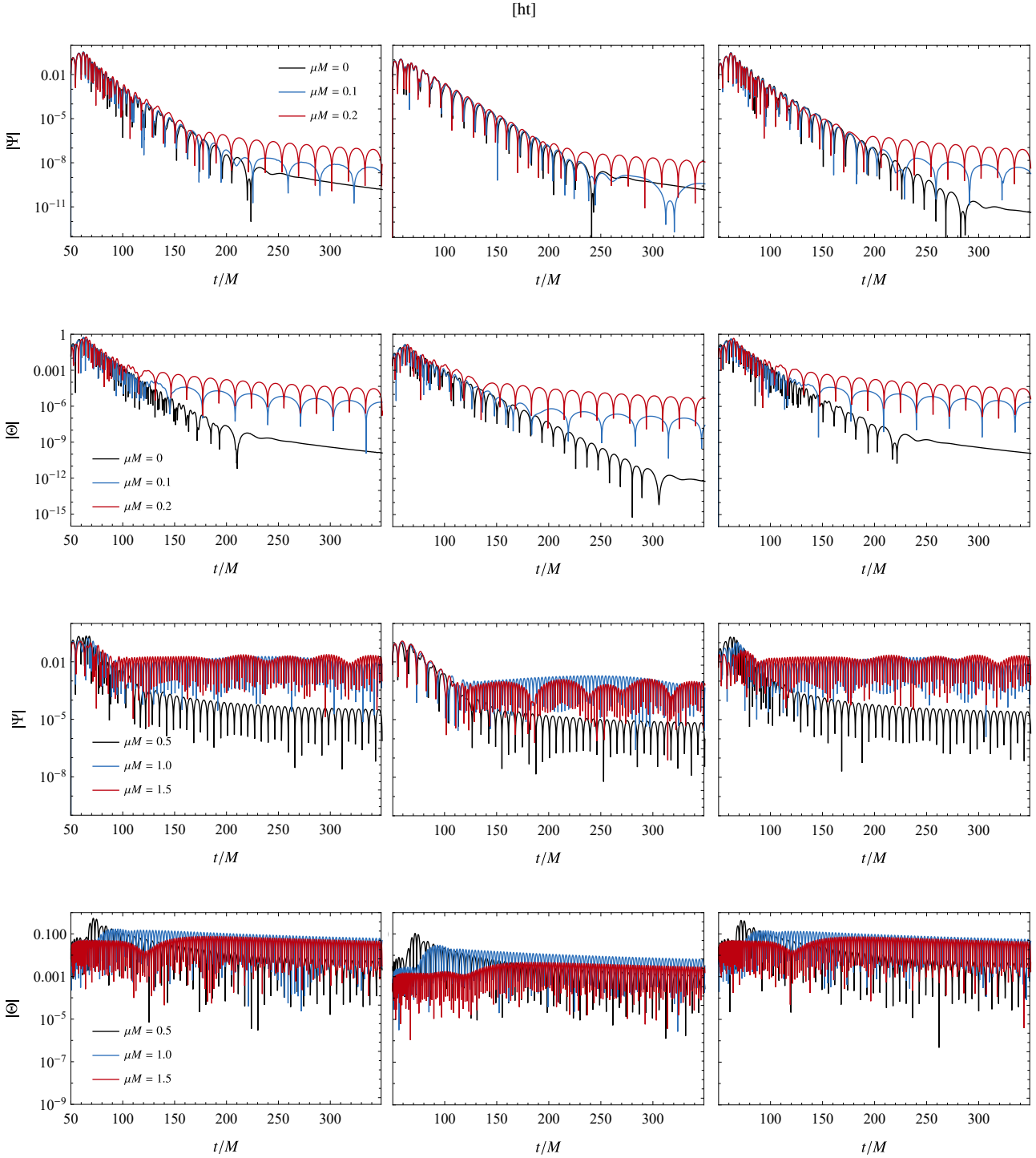


**Figure 2.** Same as Fig. 1 but for  $\tilde{\beta} = 1$  (stronger coupling). Notice that the high-frequency scalar-led mode is present in the gravitational signal for low-mass couplings  $M\mu$  but is absent when  $M\mu$  is large.

Brito R., Cardoso V., Pani P., 2020, Superradiance: New Frontiers in Black Hole Physics. Vol. 971, Springer ([arXiv:1501.06570](https://arxiv.org/abs/1501.06570)), doi:10.1007/978-3-319-19000-6  
 Cardoso V., Pani P., 2019, *Living Rev. Rel.*, 22, 4  
 Cardoso V., Yoshida S., 2005, *JHEP*, 07, 009  
 Cardoso V., Lemos J. P. S., Yoshida S., 2003, *Phys. Rev.*, D68, 084011  
 Cardoso V., Chakrabarti S., Pani P., Berti E., Gualtieri L., 2011, *Phys. Rev.*

*Lett.*, 107, 241101  
 Cardoso V., Carucci I. P., Pani P., Sotiriou T. P., 2013a, *Phys. Rev. D*, 88, 044056  
 Cardoso V., Carucci I. P., Pani P., Sotiriou T. P., 2013b, *Phys. Rev. Lett.*, 111, 111101  
 Cardoso V., Macedo C. F. B., Pani P., Ferrari V., 2016, *JCAP*, 1605, 054  
 Cardoso V., Pani P., Yu T.-T., 2017, *Phys. Rev.*, D95, 124056

Chandrasekhar S., 1983, *The Mathematical Theory of Black Holes*. Oxford University Press, New York

Christiansen O., Jiménez J. B., Mota D. F., 2020

Conlon J. P., Herdeiro C. A. R., 2018, *Phys. Lett.*, B780, 169

Damour T., Deruelle N., Ruffini R., 1976, *Lett. Nuovo Cim.*, 15, 257

Dendy R. O., 1989, *Plasma Dynamics*. Oxford University Press, Oxford, UK

Detweiler S. L., 1980, *Phys. Rev.*, D22, 2323

Dias O. J., Horowitz G. T., Marolf D., Santos J. E., 2012, *Class. Quant. Grav.*, 29, 235019

Dima A., Barausse E., 2020, *Class. Quant. Grav.*, 37, 175006

Dolan S. R., 2018, *Phys. Rev.*, D98, 104006

Dowling J. P., Scully M. O., DeMartini F., 1991, *Optics Communications*, 82, 415

East W. E., 2017, *Phys. Rev.*, D96, 024004

East W. E., 2018, *Phys. Rev. Lett.*, 121, 131104

East W. E., Pretorius F., 2017, *Phys. Rev. Lett.*, 119, 041101

Endlich S., Penco R., 2017, *JHEP*, 05, 052

Frolov V. P., Krtous P., Kubiznak D., Santos J. E., 2018, *Phys. Rev. Lett.*, 120, 231103

Fukuda H., Nakayama K., 2020, *JHEP*, 01, 128

Gibbons G., 1975, *Commun.Math.Phys.*, 44, 245

Goldreich P., Julian W. H., 1969, *ApJ*, 157, 869

Haroche S., Kleppner D., 1989, *Physics Today*, 42, 24

Haroche S., Raimond J., 1985, *Academic Press*, pp 347 – 411, [doi:https://doi.org/10.1016/S0065-2199\(08\)60271-7](https://doi.org/10.1016/S0065-2199(08)60271-7), <http://www.sciencedirect.com/science/article/pii/S0065219908602717>

Hod S., Piran T., 1998, *Phys. Rev. D*, 58, 044018

Hora H., 1991, *Plasmas at High Temperature and Density*. Springer, Heidelberg

Ikeda T., Brito R., Cardoso V., 2019, *Phys. Rev. Lett.*, 122, 081101

Jackson J. D., 1999, *Classical electrodynamics*, 3rd ed. edn. Wiley, New York, NY, <http://cdsweb.cern.ch/record/490457>

Jai-akson P., Chatrabhuti A., Evnin O., Lehner L., 2017, *Phys. Rev.*, D96, 044031

Johnston M., Ruffini R., Zerilli F., 1973, *Phys. Rev. Lett.*, 31, 1317

Kaw P., Dawson J., 1970, *Physics of Fluids*, 13, 472

Koyama H., Tomimatsu A., 2001, *Phys. Rev. D*, 64, 044014

Koyama H., Tomimatsu A., 2002, *Phys. Rev. D*, 65, 084031

Kulsrud R., Loeb A., 1992, *Phys. Rev. D*, 45, 525

Liebling S. L., Palenzuela C., 2016, *Phys. Rev.*, D94, 064046

Liu L., Guo Z.-K., Cai R.-G., Kim S. P., 2020, *Phys. Rev. D*, 102, 043508

Macedo C. F., 2018, *Phys. Rev. D*, 98, 084054

Max C., Perkins F., 1971, *Physical Review Letters*, 27, 1342

Molina C., Pani P., Cardoso V., Gualtieri L., 2010, *Phys. Rev.*, D81, 124021

Okounkova M., 2020, *Phys. Rev. D*, 102, 084046

Okounkova M., Stein L. C., Scheel M. A., Hemberger D. A., 2017, *Phys. Rev.*, D96, 044020

Pani P., 2013, *Int. J. Mod. Phys.*, A28, 1340018

Pani P., Loeb A., 2013, *Phys.Rev.*, D88, 041301

Pani P., Cardoso V., Gualtieri L., Berti E., Ishibashi A., 2012a, *Phys. Rev. Lett.*, 109, 131102

Pani P., Cardoso V., Gualtieri L., Berti E., Ishibashi A., 2012b, *Phys.Rev.*, D86, 104017

Peters P., 1964, *Phys. Rev.*, 136, B1224

Plascencia A. D., Urbano A., 2018, *JCAP*, 1804, 059

Price R. H., 1972, *Phys. Rev.*, D5, 2419

Ramazano glu F. M., Pretorius F., 2016, *Phys. Rev. D*, 93, 064005

Regge T., Wheeler J. A., 1957, *Phys. Rev.*, 108, 1063

Ruderman M. A., Sutherland P. G., 1975, *ApJ*, 196, 51

Siemonsen N., East W. E., 2020, *Phys. Rev.*, D101, 024019

Will C. M., 2014, *Living Rev. Rel.*, 17, 4

Witek H., Cardoso V., Ishibashi A., Sperhake U., 2013, *Phys.Rev.*, D87, 043513

Witek H., Gualtieri L., Pani P., Sotiriou T. P., 2019, *Phys. Rev. D*, 99, 064035

Yagi K., Stein L. C., 2016, *Class. Quant. Grav.*, 33, 054001

Yunes N., Pani P., Cardoso V., 2012, *Phys. Rev. D*, 85, 102003

Zajaček M., et al., 2019, *J. Phys. Conf. Ser.*, 1258, 012031

Zel'dovich Y. B., 1971, *Pis'ma Zh. Eksp. Teor. Fiz.*, 14, 270 [*JETP Lett.* 14, 180 (1971)]

Zel'dovich Y. B., 1972, *Zh. Eksp. Teor. Fiz.*, 62, 2076 [*Sov.Phys. JETP* 35, 1085 (1972)]

Zerilli F., 1970, *Phys. Rev. D*, 2, 2141

Zerilli F. J., 1974, *Phys. Rev.*, D9, 860

Zhu R., Osburn T., 2018, *Phys. Rev.*, D97, 104058

Zilhão M., Cardoso V., Herdeiro C., Lehner L., Sperhake U., 2012, *Phys. Rev.*, D85, 124062

Zilhão M., Cardoso V., Herdeiro C., Lehner L., Sperhake U., 2014, *Phys. Rev.*, D89, 044008

## APPENDIX A: RINGDOWN FROM THE COLLISION OF CHARGED BHs

We can gain some insight into the ringdown stage of the collision of two electrically charged BH by looking at the simplified problem of a charged particle plunging into a charged BH. This setup was explored in previous work (Zerilli 1974; Johnston et al. 1973; Cardoso et al. 2003, 2016). Here we outline the main aspects to illustrate that – neglecting EM-plasma interactions – the ringdown stage is contaminated by other modes, namely the EM one.

Consider a charged particle falling radially into a charged BH. Due to the symmetry of the problem, the particle only excites the polar sector of the perturbations. The metric, therefore, can be written as

$$g_{ab} = g_{ab}^{(0)} + h_{ab}, \quad (\text{A1})$$

with  $g_{ab}^{(0)} = \text{diag}\{-f, f^{-1}, r^2, r^2 \sin^2 \theta\}$ , with  $f = 1 - 2M/r + Q^2/r^2$ , where  $M$  is the mass and  $Q$  the BH charge. The metric perturbation  $h_{ab}$  induced by the falling particle can be decomposed into spherical harmonics. We can study the perturbation in the Regge-Wheeler gauge (Regge & Wheeler 1957),

$$h_{ab} = \begin{pmatrix} e^\nu H_0 & H_1 & 0 & 0 \\ H_1 & e^{-\nu} H_2 & 0 & 0 \\ 0 & 0 & r^2 K & 0 \\ 0 & 0 & 0 & r^2 \sin^2 \theta K \end{pmatrix} Y_{lm}(\theta, \phi), \quad (\text{A2})$$

with  $Y_{lm}(\theta, \phi)$  being the standard spherical harmonics. The electromagnetic perturbations can be also expanded in harmonics, being described by the perturbation of the vector potential  $\delta A_a = (\delta A_0, \delta A_1, 0, 0) Y_{lm}$ . Finally, one can also decompose the particle stress-energy tensor into tensorial harmonics as (Zerilli 1970)

$$T_{ab} = \begin{pmatrix} A_0 & \frac{i}{\sqrt{2}} A_{(1)} & 0 & 0 \\ \frac{i}{\sqrt{2}} A_{(1)} & A & 0 & 0 \\ 0 & 0 & 0 & 0 \\ 0 & 0 & 0 & 0 \end{pmatrix} Y_{lm}, \quad (\text{A3})$$

where the radial functions  $A_0$ ,  $A_{(1)}$ , and  $A$  depend on the particle's motion. By plugging this into Einstein-Maxwell equation and upon linearization, we can find equations describing the perturbations of the metric perturbations and of the vector potential. We direct the reader to Ref. (Cardoso et al. 2016) for more details.

By considering plunging processes, we can investigate the waveform emitted during the collision. The waveform presents the characteristic ringdown in which the signal oscillates according to the quasinormal mode frequency of the BH decaying expo-

nentially in time. In Fig. A1 we show the GWs emitted<sup>5</sup> from the collision of a BH with charge  $Q$  with a charged particle with charge  $q = -Q$ . The left panel shows the case of relatively small charges ( $Q = -q = 0.1M$ ), in which the ringdown contains basically the gravitational-led fundamental quasinormal mode of the central Reissner-Nordstrom BH. For higher charges (right panel of Fig. A1, in which  $Q = -q = 0.9M$ ), the signal is less regular, being contaminated by additional modes. The waveform may be thought as the superposition of two types of modes: the standard gravitational-led one and the EM-led one, which is sufficiently excited in the high-charge (i.e. large-coupling) case and it therefore appears in the GW signal. In fact, by considering an expansion of the form

$$K(t) \approx \sum_n K_n e^{-i\omega_n t}, \quad (\text{A4})$$

one can use the Prony method to find that the expansion is predominantly given by the frequencies of the fundamental gravitational-led (with frequency  $\omega M = 0.414 - 0.088i$ ) and EM ( $\omega M = 0.620 - 0.096i$ ) modes. The superposition of modes can also be seen by analyzing the power spectrum of the GW flux, as shown in Fig. A2, where the vertical lines mark the real parts gravitational-led and the EM-led modes.

The latter case is what one may expect when the BH is isolated, without the presence of plasma. As discussed in the main text, the main effect of the EM-plasma coupling is to provide an effective mass term for the EM mode, suppressing its excitation in the GW signal.

This paper has been typeset from a  $\text{\LaTeX}$  file prepared by the author.

<sup>5</sup> Note that here we are using the  $K$  function of Eq. (A2) to represent the GW. We remark that  $K$  is related to the (gauge-invariant) Zerilli function asymptotically by a derivative.

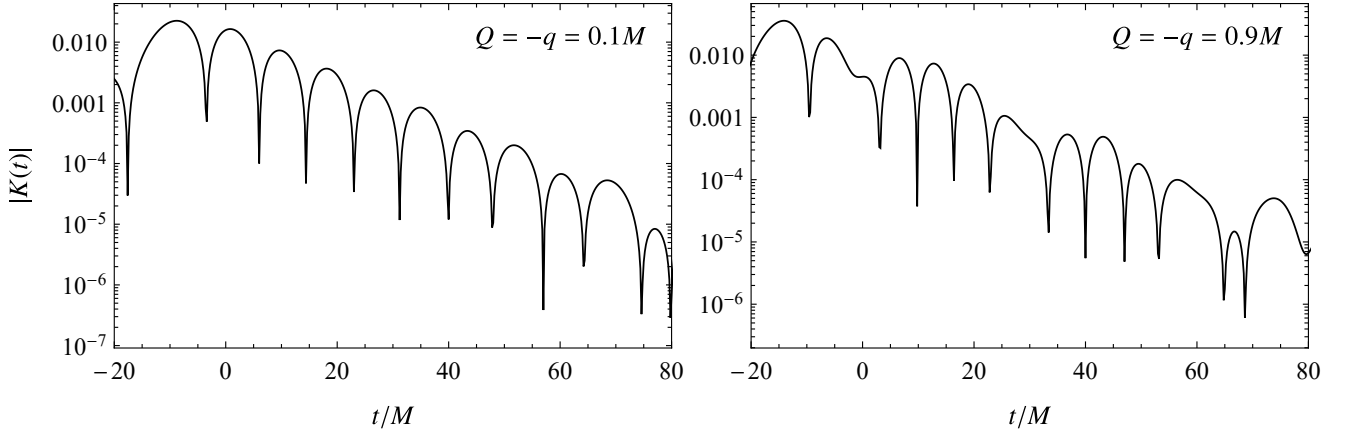


**Figure A1.** Ringdown produced by the collision of charged BH with a charged particle (taking only the dominant quadrupole term). The left and right panels correspond to the case of relatively small and large charges, respectively. In the former case the signal is essentially dominated by the gravitational-led mode, whereas for highly charged configurations the signal is contaminated by the additional EM-led mode.

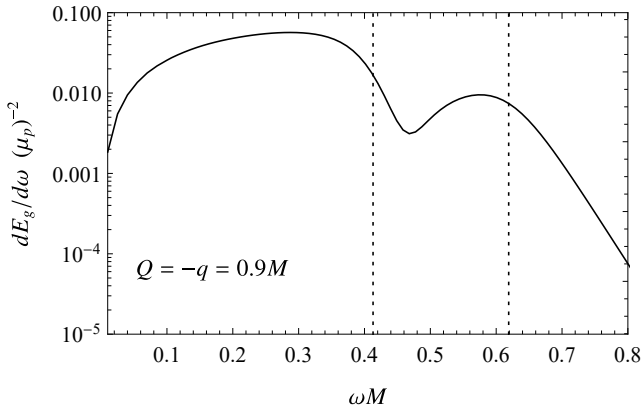


**Figure A2.** Gravitational energy flux as a function of the frequency  $\omega$  for the plunge of a particle with mass  $\mu_p$  and charge  $q$  into a BH with charge  $Q$  (taking only the dominant quadrupole term). The vertical dotted lines mark the real part of the gravitational and EM fundamental modes of the corresponding Reissner-Nordstrom BH.